Available online at www.sciencedirect.com
ScienceDirect
International Journal of Mechanical Sciences 48 (2006) 1464–1470
International Journal of MECHANICAL SCIENCES
www.elsevier.com/locate/ijmecsci

Stone–Wales transformation: Precursor of fracture in carbon nanotubes

J. Song[a], H. Jiang[c], D.-L. Shi[b], X.-Q. Feng[b], Y. Huang[a,*], M.-F. Yu[a], K.-C. Hwang[b]

[a]*Department of Mechanical Science and Engineering, University of Illinois, 1206 W. Green Street, Urbana, IL 61801, USA*
[b]*Department of Engineering Mechanics, Tsinghua University, Beijing 100084, China*
[c]*Department of Mechanical and Aerospace Engineering, Arizona State University, Tempe, AZ 85287-6106, USA*

Received 14 October 2005; received in revised form 3 February 2006; accepted 29 March 2006
Available online 22 August 2006

Abstract

The fracture strain of carbon nanotubes (CNTs) obtained by molecular dynamics is about 30%, which is much higher than the experimental results (10–13%). The present study shows that this difference results mainly from defects in CNTs. As the tensile strain reaches a few percent, defects are nucleated in the form of Stone–Wales transformation (90° rotation of a bond). A bond in the vicinity of rotated bond breaks as the tensile strain reaches about 13%, which agrees well with the experimental results. Therefore, the Stone–Wales transformation is the precursor of CNT fracture.
© 2006 Elsevier Ltd. All rights reserved.

Keywords: Stone–Wales transformation; Bond breakage; Fracture; Carbon nanotube

1. Introduction

Carbon nanotubes (CNTs) possess superior properties and have many potential applications such as nanoelectronics, nanoscale electromechanical systems (NEMS), and nanocomposites. The mass density of CNTs is only one-sixth of that for steel, but their Young's modulus is six times higher than steel and is of the order 1 TPa; the strength of CNTs is of the order 50 GPa, which is two orders of magnitude higher than that of steel (e.g., see the review articles, [1–5]).

The atomistic studies have shown that CNTs have large tensile fracture strain around 30% [6–8] or even higher [9]. The continuum theory of Zhang et al. [10] and Jiang et al. [11] based on interatomic potentials for carbon [12,13] also predicts the fracture strain in the same range [14,15]. However, the experimental studies of Yu et al. [16] for multiwall CNTs found the tensile failure strain of CNTs between 10% and 13%, which is much lower than the aforementioned atomistic simulations or atomistic-based continuum studies. Most multiwall CNTs fail in a sheath-like pattern with only the outer nanotube failing. Since the van der Waals interactions between CNT walls are weak, this failure is essentially the same as that for single-wall CNTs. Yu et al. [17] also measured the failure strain of single-wall CNT bundles, and found even lower failure strains around 5–6%. Belytschko et al. [18] and Dumitrica et al. [19] showed that this discrepancy between the atomistic and experimental studies of failure strains can be attributed to the nonphysical cutoff function introduced in Brenner's [12] interatomic potential. They used a modified Morse potential to fit the Brenner potential for strain up to 10%, and predicted the failure strain between 10% and 16%, which agrees with most of Yu et al.'s [16] experimental results.

Belytschko et al. [18] introduced a weak bond in the CNT to serve as the site for bond breakage in their atomistic simulations of CNT fracture. The strength of the weak bond was 10% lower than others. The weak bond broke first upon loading, and bond breakage rapidly propagated to neighbor bonds, leading to brittle fracture of the CNT. It is unclear, however, whether the fracture strain of CNTs depends on this imperfection. It is also unclear how fracture starts in a perfect CNT without any preexisting defects.

The purpose of this paper is to study the failure of single-wall CNTs without introducing any initial imperfections.

*Corresponding author. Tel.: +1 217 265 5072; fax: +1 217 244 6534.
E-mail address: huang9@uiuc.edu (Y. Huang).

0020-7403/$ - see front matter © 2006 Elsevier Ltd. All rights reserved.
doi:10.1016/j.ijmecsci.2006.03.019

We study how fracture initiates in a perfect CNT without any preexisting defects, and compare its fracture strain with Yu et al.'s [16] experimental results. We show that, even without any preexisting defects, Stone–Wales transformation in the form of 90° rotation of a carbon bond may occur in the CNT upon loading. This bond rotation triggers bond breakage as the loading increases, i.e., *Stone–Wales transformation becomes the precursor of CNT failure*. Furthermore, bond breakage always occurs before any atomic bond length reaches the cutoff distance (0.17 nm) in Brenner's [12] interatomic potential such that the Stone–Wales transformation, not the nonphysical cutoff function in the interatomic potential, is responsible for the discrepancy between the atomistic and experimental studies of failure strain.

The paper is outlined as follows. We develop a hybrid atomistic/continuum model in Section 2. The atomistic model is used for atoms near the defect, while the continuum theory [10] established from the interatomic potential for carbon [12] is used for atoms far away from the defect where the deformation is relatively uniform. The critical strain for bond breakage following Stone–Wales transformation in a CNT subject to tension is presented in Section 3, and it agrees well with the experimental results [16].

2. A hybrid atomistic/continuum model

2.1. The empirical interatomic potential for carbon

The empirical interatomic potential established by Brenner [12] for carbon takes the form

$$V = V_R(r_{ij}) - \bar{B}_{ij} V_A(r_{ij}), \tag{1}$$

where r_{ij} is the bond length; V_R and V_A are the repulsive and attractive pair terms, respectively, and $\bar{B}_{ij}$ represents the multi-body coupling which depends on neighbor atoms through the bond angle. The detailed expressions of V_R, V_A and $\bar{B}_{ij}$ and the parameters involved can be found in Brenner [12] or in Zhang et al. [10,15]. The potential involves a cutoff function, which comes into play once the bond length exceeds 0.17 nm. However, the cutoff function is irrelevant in the present study since the Stone–Wales transformation and bond breakage occur before the cutoff distance (0.17 nm) is reached.

2.2. Atomistic-based continuum model for deformed CNTs

For a perfect CNT prior to deformation, the atom positions can be determined by molecular mechanics (i.e., energy minimization). Such an approach, however, is inefficient for a large system with many atoms. Jiang et al. [11] established an efficient method to determine the atom positions on a perfect CNT prior to deformation via energy minimization with respect to only five parameters (three bond lengths and two angles).

For a perfect CNT subject to tension, the atom positions on the CNT are determined by the atomistic-based continuum theory [10,11]. The deformation gradient $\boldsymbol{F} = \partial \boldsymbol{x}/\partial \boldsymbol{X}$ characterizes the deformation of a material point in the continuum analysis, where the material point represents atoms that undergo locally uniform deformation, and $\boldsymbol{X}$ and $\boldsymbol{x}$ denote positions of the material point prior to and after deformation, respectively. For a CNT subject to tension, the deformed CNT remains to have a circular cross-section such that the deformation gradient $\boldsymbol{F}$ is intrinsically two-dimensional. Arroyo and Belytschko [20] and Jiang et al. [11] accounted for the effect of CNT curvature in the continuum model based on the interatomic potential.

Let $\boldsymbol{r}_{ij}^{(0)}$ denote the position vector from atom i to atom j prior to deformation. For a material point subject to the deformation gradient $\boldsymbol{F}$, the position vector $\boldsymbol{r}_{ij}^{(0)}$ becomes $\boldsymbol{r}_{ij} = \boldsymbol{F} \cdot \boldsymbol{r}_{ij}^{(0)}$ after deformation. Using the Cauchy–Born rule [21,22] which equates the strain energy at continuum level to energy stored in atomic bonds, we obtain the strain energy density W as a function of deformation gradient $\boldsymbol{F}$, i.e., $W = W(\boldsymbol{F})$. Such an approach to obtain W from the interatomic potential, however, is limited to materials with a centrosymmetric atomic structure since the centrosymmetry together with $\boldsymbol{r}_{ij} = \boldsymbol{F} \cdot \boldsymbol{r}_{ij}^{(0)}$ ensure the equilibrium of atoms [10,15,23–25].

A CNT, however, does not possess centrosymmetry. As shown in Fig. 1(a), a CNT prior to deformation can be decomposed to two sub-lattices marked by open and solid circles, respectively. Each sublattice (e.g., solid circles) is triangular and possesses centrosymmetry. Once the deformation is imposed, the Cauchy–Born rule discussed above can be applied to each sub-lattice, but two sub-lattices may undergo a shift vector $\boldsymbol{\zeta}$, as shown in Fig. 1(b). This shift vector $\boldsymbol{\zeta}$ plays the role of relaxing atoms between two sub-lattices in order to ensure equilibrium of atoms [10,23–25]. The position vector $\boldsymbol{r}_{ij}$ between atoms i and j from two different sub-lattices then becomes

$$\boldsymbol{r}_{ij} = \boldsymbol{F} \cdot \boldsymbol{r}_{ij}^{(0)} + \boldsymbol{\zeta}, \tag{2}$$

and their distance is

$$r_{ij} = \|\boldsymbol{r}_{ij}\| = \sqrt{\boldsymbol{\zeta} \cdot \boldsymbol{\zeta} + 2\boldsymbol{\zeta} \cdot \boldsymbol{F} \cdot \boldsymbol{r}_{ij}^{(0)} + \boldsymbol{r}_{ij}^{(0)} \cdot \boldsymbol{F}^{\mathrm{T}} \cdot \boldsymbol{F} \cdot \boldsymbol{r}_{ij}^{(0)}}. \tag{3}$$

The energy stored in atomic bonds obtained from the interatomic potential now depends on both $\boldsymbol{F}$ and $\boldsymbol{\zeta}$. The Cauchy–Born rule then gives the strain energy density W in the continuum analysis in terms of $\boldsymbol{F}$ and $\boldsymbol{\zeta}$ via the interatomic potential, i.e., $W = W(\boldsymbol{F},\boldsymbol{\zeta})$.

The shift vector $\boldsymbol{\zeta}$ is determined by energy minimization which is equivalent to equilibrium of atoms [10,11], i.e.,

$$\frac{\partial W}{\partial \boldsymbol{\zeta}} = 0. \tag{4}$$

This is an implicit equation to determine the shift vector $\boldsymbol{\zeta}$ in terms of $\boldsymbol{F}$, i.e., $\boldsymbol{\zeta} = \boldsymbol{\zeta}(\boldsymbol{F})$. The strain energy

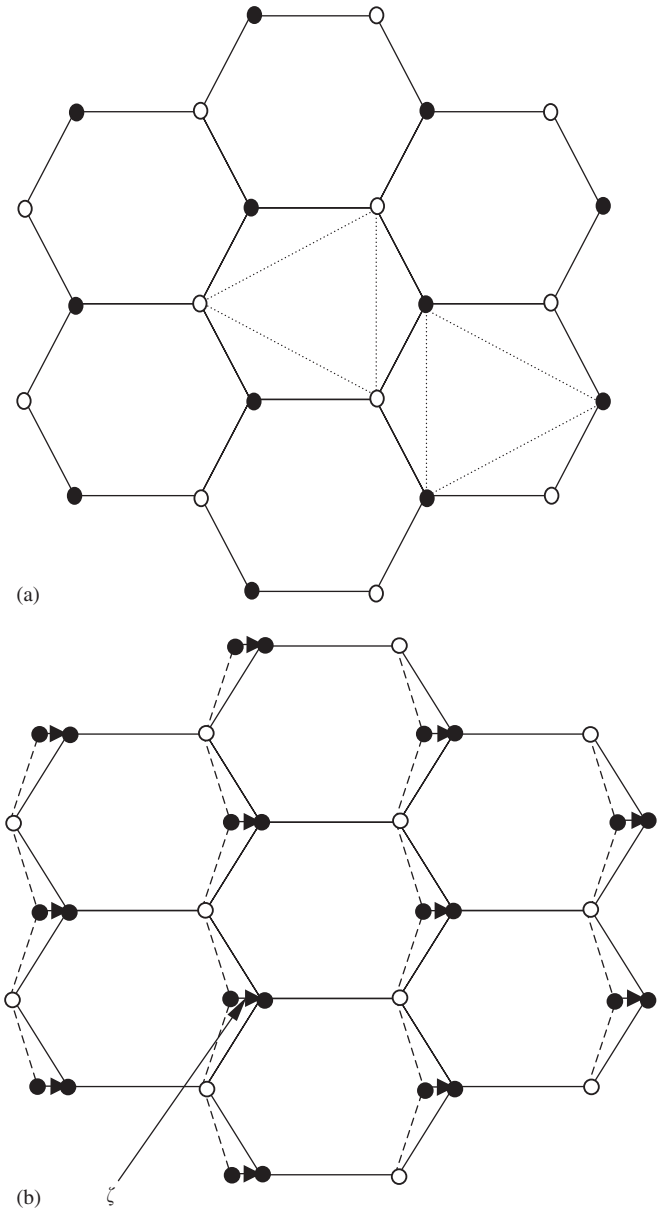

Fig. 1. (a) The decomposition of a hexagonal lattice to two triangular sub-lattices, which are denoted by the dotted triangles; and (b) a shift vector ζ between two sub-lattices is introduced to ensure the equilibrium of atoms. The solid and dashed lines denote the lattice structures with and without the shift vector ζ, respectively.

density then becomes

$$W = W[\boldsymbol{F}, \boldsymbol{\zeta}(\boldsymbol{F})]. \tag{5}$$

The second Piola–Kirchhoff stress $\boldsymbol{T}$ is the work conjugate of Green strain $\boldsymbol{E} = \frac{1}{2}(\boldsymbol{F}^{\mathrm{T}} \cdot \boldsymbol{F} - \boldsymbol{I})$, i.e., $\boldsymbol{T} = \partial W/\partial \boldsymbol{E}$, where $\boldsymbol{F}^{\mathrm{T}}$ is the transpose of $\boldsymbol{F}$ and $\boldsymbol{I}$ is the second-order identity tensor. For a CNT subject to the tensile strain E_{ZZ} in the tube axial direction Z, the uniaxial tension condition gives

$$T_{\theta\theta} = \frac{\partial W}{\partial E_{\theta\theta}} = 0, \tag{6}$$

where $E_{\theta\theta}$ is the strain in the circumferential direction. Eq. (6) gives $E_{\theta\theta}$ in terms of E_{ZZ}.

2.3. A hybrid atomistic/continuum model for Stone–Wales transformation

The atomistic-based continuum model described above represents the collective behavior of atoms such that it cannot be used to characterize an individual atomic bond as in Stone–Wales transformation which involves the 90° rotation of a carbon bond. However, the effect of Stone–Wales transformation is rather localized and limited to atoms in the vicinity of the rotated bond. Atoms far away from the rotated bond undergo relatively uniform deformation such that the atomistic-based continuum theory is still applicable. Jiang et al. [26] developed a hybrid atomistic/continuum model to couple molecular mechanics (for atoms near the rotated bond) with the atomistic-based continuum theory to study Stone–Wales transformation in CNTs. Their analysis, however, was limited to the cylindrical configuration of the CNT even after the Stone–Wales transformation. We remove this limitation in the present study, and extend the hybrid atomistic/continuum model to study bond breakage in the next section.

Figs. 2(a) and (b) show schematic diagrams of the hybrid atomistic/continuum model without and with the Stone–Wales transformation, respectively. Even though the planar lattices are shown in Figs. 2(a) and (b), all calculations are done for the three-dimensional configuration of the CNT. As the strain in the CNT reaches a critical value, a carbon bond rotates 90° (Stone–Wales transformation) forming two pentagons and two heptagons which is called the 5–7–7–5 ring pair. After the bond rotation, atoms do not sit on a cylinder anymore, which is different from Jiang et al. [26].

The atoms are divided to two groups as shown in Fig. 2(a):

(i) Atoms far away from the rotated bond are marked by open and solid circles which are consistent with Fig. 1 to distinguish atoms from two sub-lattices. Atoms in this group undergo relatively uniform deformation since the effect of bond rotation is rather localized. Their positions are determined by the atomistic-based continuum model in Section 2.2, i.e., are given in terms of the atom positions prior to deformation (Section 2.2) and the strain E_{ZZ} [The strain $E_{\theta\theta}$ and shift vector ζ are related to E_{ZZ} via Eqs. (4) and (6)].

(ii) Atoms in the vicinity of the rotated bond are marked by shaded circles. Atoms in this group undergo nonuniform deformation due to bond rotation. Their positions are to be determined by molecular mechanics to minimize the total energy of the system once atom positions in group (i) are known. The conjugate gradient method provided by the IMSL program [27] is adopted to minimize the total energy.

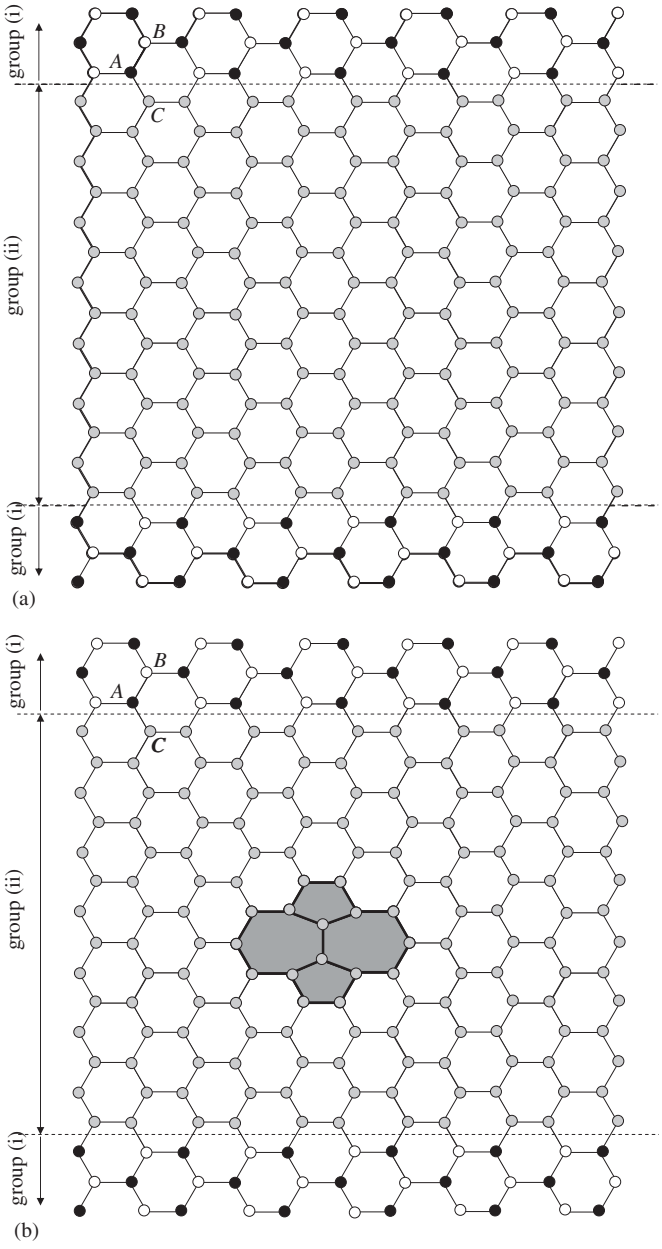

Fig. 2. A hybrid atomistic/continuum model for studying the Stone–Wales transformation: (a) before and (b) after bond rotation, where the atoms around the rotated bond are highlighted.

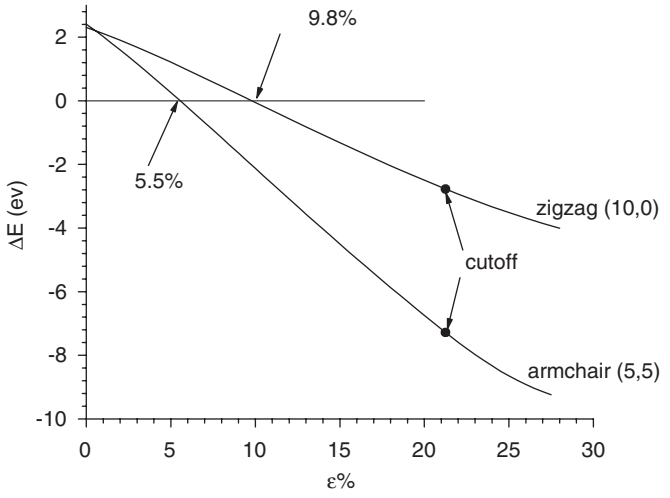

Fig. 3. The energy difference ΔE versus the tensile strain ε for armchair (5,5) and zigzag (10,0) carbon nanotubes. Here $\Delta E = E - E_{perfect}$ is the difference between the energy for systems with and without Stone–Wales transformation.

It is important to point out that, even though atoms are divided to two groups, the total energy of the system cannot be divided because of the multi-body nature of atomistic interactions in carbon [12]. For example, even though atoms A and B are both in group (i) as shown in Fig. 2(a), the energy stored in the AB bond depends on the position of atom C in group (ii). Therefore, it is important to account for the energy stored in all atomic bonds that is influenced by atoms in group (ii).

We use the above hybrid atomistic/continuum model to calculate the energy $E_{perfect}$ in the system without bond rotation (Fig. 2(a)), and energy E with 90° rotation of a bond (Fig. 2(b)). Fig. 3 shows the difference in energy with and without bond rotation, $\Delta E = E - E_{perfect}$, versus the tensile strain ε ($= F_{ZZ} - 1$) for the (5,5) armchair CNT and (10,0) zigzag CNT. The perfect structure is stable at small strain because the energy E is higher than $E_{perfect}$. As the strain increases, ΔE decreases and eventually becomes negative such that the configuration with the rotated bond (Fig. 2(b)) becomes energetically favorable and Stone–Wales transformation may occur. The critical strain ε_{SW} for Stone–Wales transformation is determined by $\Delta E = 0$, which gives the critical strains $\varepsilon_{SW} = 5.5\%$ for the (5,5) armchair CNT, and $\varepsilon_{SW} = 9.8\%$ for the (10,0) zigzag CNT. These are both larger than the critical strains reported by Jiang et al. [26] (which were limited to the cylindrical configuration after bond rotation), but they agree well with Nardelli et al.'s [28] molecular dynamic simulation results (about 5% for armchair and 10% for zigzag CNTs).

The dot on each curve in Fig. 3 denotes the critical point at which the maximum bond length reaches the cutoff distance (0.17 nm) in Brenner's [12] interatomic potential. Therefore, the Stone–Wales transformation occurs before the cutoff distance is reached such that the cutoff distance has no effect on the Stone–Wales transformation.

There must be sufficient number of layers of atoms in group (ii) (in the vicinity of the rotated bond) in order to ensure the energy E and the critical strain ε_{SW} are accurate. We have compared the results for 9, 17, 23 and 25 layers of atoms in group (ii) and have found that the results for 23 layers have converged.

3. Bond breakage

We extend the hybrid atomistic/continuum model to study bond breakage triggered by Stone–Wales transformation. Fig. 4(a) shows the same schematic diagram of an

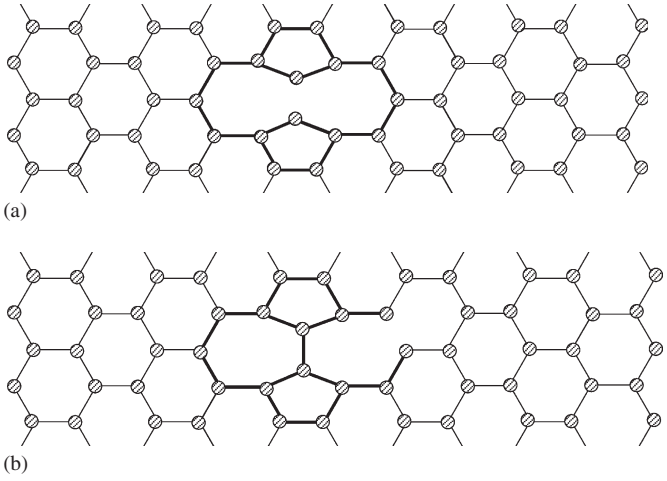

Fig. 4. Schematic diagram of bond breakage following Stone–Wales transformation; (a) breakage of the rotated bond; (b) bond breakage in the vicinity of rotated bond.

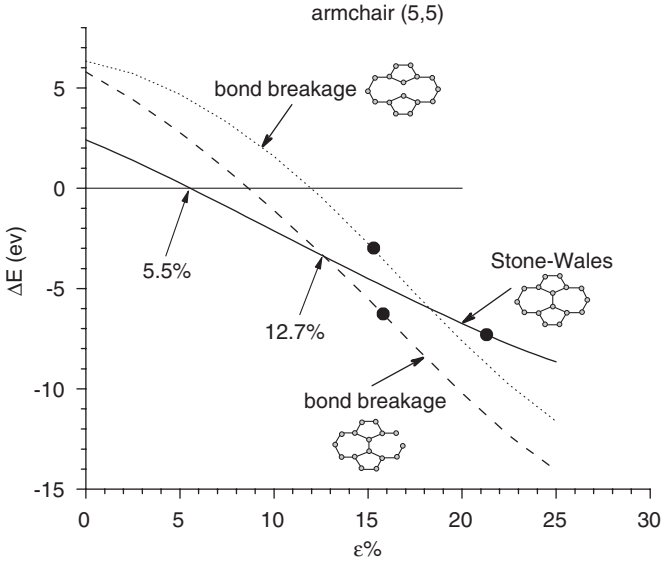

Fig. 5. The energy difference $\Delta E = E - E_{perfect}$ versus the tensile strain ε for the armchair (5,5) carbon nanotube, where $E_{perfect}$ is the energy for the system without any defects, and E is the energy for system with Stone–Wales transformation and/or bond breakage.

armchair CNT as Fig. 2(b) after Stone–Wales transformation except that the rotated bond breaks. Let E denote the energy of this system (Fig. 4(a)), and $\Delta E = E - E_{perfect}$ the energy difference with respect to the perfect structure shown in Fig. 2(a). The breakage of the rotated bond occurs when the above ΔE (for both bond rotation and breakage) becomes less than the energy difference in Fig. 3 for Stone–Wales transformation only.

The bond breakage, however, may occur at one of the other bonds in the vicinity of the rotated bond as illustrated in Fig. 4(b), if the breakage of such a bond gives lower energy than that for the breakage of the rotated bond (Fig. 4(a)). Fig. 5 shows the energy difference $\Delta E = E - E_{perfect}$ versus the tensile strain ε for (5,5) armchair CNTs with three possible imperfections,

(i) Stone–Wales transformation only as illustrated in Fig. 2(b);
(ii) Stone–Wales transformation and the breakage of rotated bond as illustrated in Fig. 4(a);
(iii) Stone–Wales transformation and bond breakage in the vicinity of rotated bond as illustrated in Fig. 4(b).

The energy difference ΔE is always positive for strain less than 5.5% such that the perfect structure (Fig. 2(a)) is stable at small strain. Once the strain exceeds 5.5% (but less than 12.7%), ΔE becomes negative for Stone–Wales transformation, though the corresponding curve is still lower than the other two for bond breakage. Therefore, Stone–Wales transformation (without bond breakage) becomes more energetically favorable. Once the strain reaches 12.7%, the curve for Stone–Wales transformation intercepts that for bond breakage in the vicinity of rotated bond (Fig. 4(b)). The bond breakage (following Stone–Wales transformation) is more energetically favorable for strain larger than 12.7%, and may occur in the vicinity of rotated bond. The rotated bond does not break because the corresponding curve is always above that for bond breakage in the vicinity of rotated bond (Fig. 4(b)). In fact, bond breakage shown in Fig. 4(b) occurs at the smallest strain among all possible bonds in the vicinity of rotated bond.

The CNT failure is brittle at low temperature (e.g., Ref. [19,28]) such that the bond breakage rapidly propagates and leads to fracture of the CNT. The strain for bond breakage (12.7%) is much smaller than that (around 30%) reported in molecular dynamics studies [6–8], but it agrees well with the experimentally measured fracture strain 10–13% [16]. These molecular dynamics simulations involve high strain rate, and do not allow sufficient time for relaxation, which prevents the Stone–Wales transformation and leads to large fracture strain. The results in Fig. 5 suggest that bond breakage triggered by Stone–Wales transformation may occur at a smaller strain of 12.7% in the (5,5) armchair CNT.

Similar to Fig. 3, the dot on each curve in Fig. 5 denotes the critical strain at which the maximum bond length reaches the cutoff distance (0.17 nm) in Brenner's [12] interatomic potential. Bond breakage occurs before the cutoff distance is reached such that the cutoff distance has no effect on fracture of CNTs.

Fig. 6 shows the energy difference $\Delta E = E - E_{perfect}$ versus strain ε for (10,0) zigzag CNTs with (i) Stone–Wales transformation only; (ii) Stone–Wales transformation and the breakage of rotated bond as illustrated in Fig. 7(a); and (iii) Stone–Wales transformation and bond breakage in the vicinity of rotated bond as illustrated in Fig. 7(b). Stone–Wales transformation occurs at 9.8% for the (10,0) zigzag CNT while bond breakage occurs at 13.3% in the vicinity of rotated bond. Similar to armchair CNTs, the rotated bond does not break. The configuration

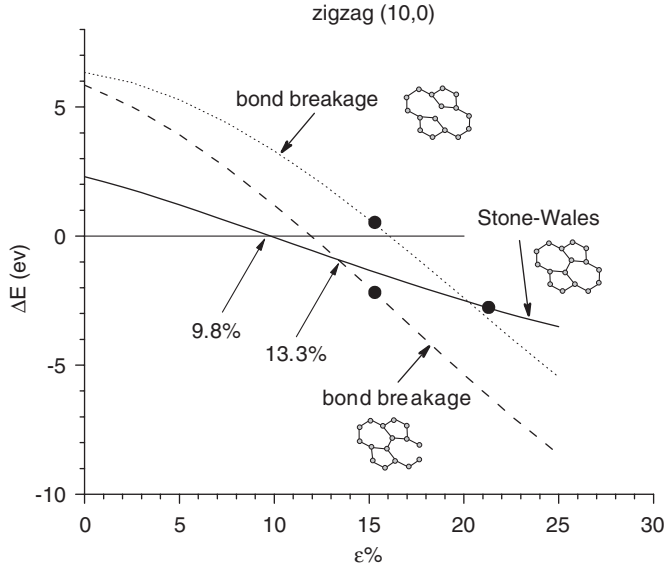

Fig. 6. The energy difference $\Delta E = E - E_{perfect}$ versus the tensile strain ε for the zigzag (10,0) carbon nanotube, where $E_{perfect}$ is the energy for the system without any defects, and E is the energy for system with Stone–Wales transformation and/or bond breakage.

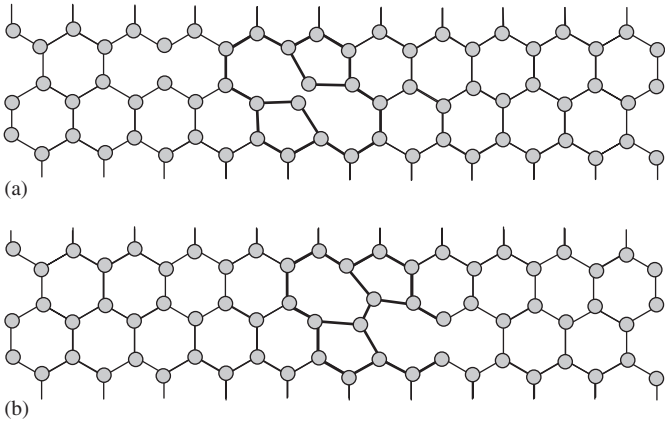

Fig. 7. Schematic diagram of bond breakage following Stone–Wales transformation; (a) breakage of the rotated bond; (b) bond breakage in the vicinity of rotated bond.

shown in Fig. 7(b) gives the lowest strain for bond breakage in the vicinity of rotated bond. The critical strain (9.8%) for Stone–Wales transformation in zigzag (10,0) CNT is much higher than its counterpart (5.5%) for (5,5) armchair CNT, but the strains for bond breakage are rather close (12.7% versus 13.3%), and both agree well with the fracture strain reported in Yu et al.'s [16] experiments.

4. Concluding remarks

We have used a hybrid atomistic/continuum model to study the Stone–Wales transformation and bond breakage in carbon nanotubes (CNTs) subject to tension. It is shown that bond breakage occurs after the Stone–Wales transformation, and the failure strain is about 13%, which is much smaller than the fracture strain (around 30%) reported in molecular dynamics studies, but it agrees well with the experimental results. Therefore, the Stone–Wales transformation is the precursor of CNT fracture. In other words, bond breakage does not occur directly in a perfect CNT which requires 30% strain. Instead, it follows Stone–Wales transformation and occurs at only 13% strain.

Acknowledgments

YH acknowledges the support from NSF (Grants 00-99909, 01-03257, and 03-28162 via the Nano-CEMMS Center at UIUC), Office of Naval Research (Grant N00014-01-1-0205, Program Manager Dr. Y.D.S. Rajapakse), and NSFC. KCH. and XQF acknowledge support from NSFC and the Ministry of Education, China.

References

[1] Ruoff RS, Lorents DC. Mechanical and thermal properties of carbon nanotubes. Carbon 1995;33:925–30.
[2] Govindjee S, Sackman JL. On the use of continuum mechanics to estimate the properties of nanotubes. Solid State Communications 1999;110:227–30.
[3] Yakobson BI, Avouris P. Mechanical properties of carbon nanotubes. In: Dresselhaus MS, Dresselhaus G, Avouris P, editors. Carbon nanotubes. Topics in applied physics, vol. 80. Berlin–Heidelberg, Germany: Springer; 2001 p. 287–329.
[4] Qian D, Wagner GJ, Liu WK, Yu MF, Ruoff RS. Mechanics of carbon nanotubes. Applied Mechanics Reviews 2002;55:495–533.
[5] Huang Y, Wang ZL. Mechanics of carbon nanotubes. In: Karihaloo B, Ritchie R, Milne I, editors. Comprehensive structural integrity handbook, Gerberwich W, Yang W, editors., Interfacial and nanoscale fracture, vol. 8. Amsterdam: Elsevier; 2003. p. 551–579 [chapter 8.16].
[6] Dereli G, Ozdogan C. Structural stability and energetics of single-walled carbon nanotubes under uniaxial strain. Physical Review B 2003;67:0354161–6.
[7] Ogata S, Shibutani Y. Ideal tensile strength and band gap of single-walled carbon nanotubes. Physical Review B 2003;68:1654091–4.
[8] Mielke SL, Troua D, Zhang S, Li JL, Xiao S, Car R, et al. The role of vacancy defect and holes in the fracture for carbon nanotubes. Chemical Physics Letters 2004;390:413–20.
[9] Yakobson BI, Campbell MP, Brabec CJ, Bernholc J. High strain rate fracture and C-chain unraveling in carbon nanotubes. Computational Material Science 1997;8:341–8.
[10] Zhang P, Huang Y, Geubelle PH, Klein PA, Hwang KC. The elastic modulus of single-wall carbon nanotubes: a continuum analysis incorporating interatomic potentials. International Journal of Solids and Structure 2002;39:3893–906.
[11] Jiang H, Zhang P, Liu B, Huang Y, Geubelle PH, Gao H, et al. The effect of nanotube radius on the constitutive model for carbon nanotubes. Computational Material Science 2003;28:429–42.
[12] Brenner DW. Empirical potential for hydrocarbons for use in simulating the chemical vapor deposition of diamond films. Physical Review B 1990;42:9458–71.
[13] Brenner DW, Shenderova OA, Harrison JA, Stuart SJ, Ni B, Sinnott SB. A second-generation reactive empirical bond order (rebo) potential energy expression for hydrocarbons. Journal of Physics Condensed Matter 2002;14:783–802.
[14] Zhang P, Huang Y, Gao H, Hwang KC. Fracture nucleation in single-wall carbon nanotubes under tension: a continuum analysis incorporating interatomic potentials. Journal of Applied Mechanics 2002;69:454–8.

[15] Zhang P, Jiang H, Huang Y, Geubelle PH, Hwang KC. An atomistic-based continuum theory for carbon nanotubes: analysis of fracture nucleation. Journal of the Mechanics and Physics of Solids 2004;52:977–98.
[16] Yu MF, Lourie O, Dyer MJ, Moloni K, Kelly TF, Ruoff RS. Strength and breaking mechanism of multiwalled carbon nanotubes under tensile load. Science 2000;287:637–40.
[17] Yu MF, Files BS, Arepalli S, Ruoff RS. Tensile loading of ropes of single wall carbon nanotubes and their mechanical properties. Physical Review Letters 2000;84:5552–5.
[18] Belytschko T, Xiao SP, Schatz GC, Ruoff RS. Atomistic simulations of nanotube fracture. Physical Review B 2002;65:2354301–8.
[19] Dumitrica T, Belytschko T, Yakobson BI. Bond-breaking bifurcation states in carbon nanotube fracture. Journal of Chemical Physics 2003;118:9485–8.
[20] Arroyo M, Belytschko T. An atomistic-based finite deformation membrane for single layer crystalline films. Journal of Mechanics and Physics of Solids 2002;50:1941–77.
[21] Born M, Huang K. Dynamical theory of the crystal lattices. Oxford: Oxford University Press; 1954.
[22] Milstein F. Review: theoretical elastic behaviour at large strains. Journal of Materials Science 1980;15:1071–84.
[23] Cousins C. Inner elasticity. Journal of Physics C 1978;11:4867–79.
[24] Weiner JH. Statistical Mechanics of Elasticity. New York: Wiley; 1983.
[25] Tadmor EB, Smith GS, Bernstein N, Kaxiras E. Mixed finite element and atomistic formulation for complex crystals. Physical Review B 1999;59:235–45.
[26] Jiang H, Feng XQ, Huang Y, Hwang KC, Wu PD. Defect nucleation in carbon nanotubes under tension and torsion: Stone–Wales transformation. Computer Methods in Applied Mechanics and Engineering 2004;193:3419–29.
[27] IMSL(R) Fortran 90 MP Library Version 4.01. San Ramon: McGraw-Hill; 1999.
[28] Nardelli MB, Yakobson BI, Bernholc J. Brittle and ductile behavior in carbon nanotubes. Physical Review Letters 1998;81:4656–9.